Nanoscale

COMMUNICATION

Porous Liquid Zeolites: Hydrogen Bonding-Stabilized H-ZSM-5 in Branched Ionic Liquids†

Received 00th January 20xx,
Accepted 00th January 20xx

DOI: 10.1039/x0xx00000x

www.rsc.org/

Peipei Li,[a,b,c] Hao Chen,[d] Jennifer A. Schott,[b,d] Bo Li,[e] Yaping Zheng,[c] Shannon M. Mahurin,[*,b] De-en Jiang,[*,e] Guokai Cui,[b] Xunxiang Hu,[b] Yangyang Wang,[b] Lengwan Li,[b] and Sheng Dai[*,b,d]

Porous liquids, as a newly emerging type of porous material, have great potential in gas separation and storage. However, the examples and synthetic strategies reported so far likely represent only the tip of the iceberg due to the great difficulty and challenge in engineering permanent porosity in liquid matrices. Here, by taking advantage of the hydrogen bonding interaction between the alkane chains of branched ionic liquids and the Brønsted sites in H-form zeolites, as well as the mechanical bond of the long alkyl chain of the cation penetrated into the zeolite channel at the interface, the H-form zeolites can be uniformly stabilized in branched ionic liquids to form porous liquid zeolites, which not only significantly improve their gas sorption performance, but also change the gas sorption-desorption behavior because of the preserved permanent porosity. Furthermore, such a facile synthetic strategy can be extended to fabricate other types of H-form zeolite-based porous liquids by taking advantage of the tunability of the counter-anion (e.g., NTf_2^-, BF_4^-, $EtSO_4^-$, etc.) in branched ionic liquids, thus opening up new opportunities for porous liquids for specific applications in energy and environment.

Since the idea of porous liquids was first proposed and subsequently realized, porous liquids have attracted considerable attention because of their unique fluidity with permanent porosity, and have already demonstrated promising applications in gas separation and storage, etc.[1-7] However, the development of porous liquids is just at the beginning and this specific emerging field still faces a number of challenges, such as intermolecular self-filling, easy collapse or decomposition of the organic hosts and settling of the porous nanoparticles.[7-11] Fortunately, some methods for the fabrication of porous liquids have been successfully developed, including surface engineering of hollow structures with suitable corona and canopy species,[2, 4, 12] dissolving rigid organic cage molecules in solvents that are too large to enter the pores,[3, 13-15] and liquefying metal-organic frameworks above their melting temperature.[16, 17] Those few convincing synthesis strategies should be seen as prototypes that ultimately require further expansion and development. Most importantly, economical preparation as well as scaling up of the synthesis process will also be significant and necessary for future applications.[4, 8]

Zeolites have attracted immense attention due to their highly microporous structure that could be used for varied specific applications in gas storage, separations and catalysis.[18-23] Although a vast body of work based on zeolites currently exists, nearly all of it has focused on solid zeolite crystals with almost nothing reported on the liquid states.[24-26] This is because the initial attempts to create liquid zeolites resulted in the loss of the microporous structure eliminating the primary advantage and value of the material.[27, 28] Fabrication of a porous liquid zeolite without the loss of the microporous structure will not only impart novel functionalities to zeolites but also open up a new area for future research. Unfortunately, the surface engineering of zeolites with suitable corona and canopy species seems unsuitable for the fabrication of porous liquid zeolites because of their high crystallinity, which suggests that the number of reactive sites of hydroxyl groups may not be enough to guarantee adequate corona and canopy grafting.[29] In addition, the surface engineering of zeolites can destroy their microporous structure because the small organosilane (corona) molecules will occupy the microporous structure of the zeolite.[2] The direct dispersion of zeolites in large hindered solvents seems feasible, but this promising strategy still suffers from the significant sedimentation due to aggregation of zeolites and the lack of force to counteract gravity and van der Waals attraction among zeolite nanoparticles.[9] Thus a strong liquid-particle force is needed to stabilize the dispersion of zeolites in large hindered solvents for the fabrication of porous liquid zeolites.[30]

[a] School of Advanced Materials and Nanotechnology, Xidian University, Xi'an, Shaanxi, 710071, PR China.
[b] Chemical Science Division; Materials Science and Technology Division; Center for Nanophase Materials Sciences, Oak Ridge National Laboratory, Oak Ridge, TN 37831, United States.
[c] Key Laboratory of Space Applied Physics and Chemistry, Ministry of Education; School of Natural and Applied Sciences, Northwestern Polytechnical University, Xi'an, Shaanxi, 710129, PR China.
[d] Department of Chemistry, University of Tennessee Knoxville, TN 37996, United States.
[e] Department of Chemistry, University of California, Riverside, California 92521, United States.

†Electronic Supplementary Information (ESI) available: [Experimental section, Molecular dynamics simulation and Supplementary Figures]. See DOI:10.1039/x0xx00000x

Scheme 1 Depiction of the preparation strategy for the porous liquid zeolites (H-ZSM-5-liquid/[P66614][Br]).

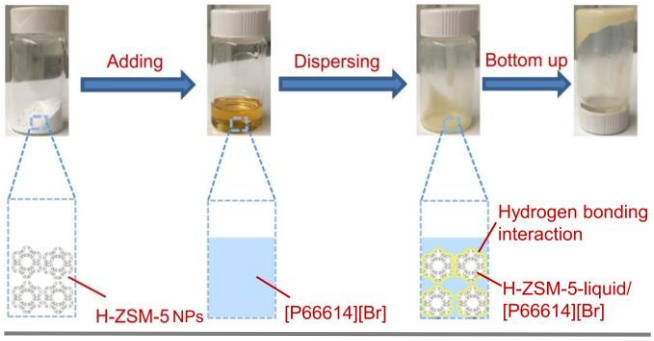

Normally, zeolites have a strong physical absorption interaction with alkanes.[31, 32] Particularly, the adsorbed alkanes have a strong hydrogen bonding interaction with the Brønsted sites that exist in H-form zeolites,[32] which explains the stabilization of H-form zeolites in ionic liquids rich in alkyl chains. In addition, the narrow window and the larger cavity of a zeolite channel can serve as a novel interfacial host for mechanical bonds which have been conventionally explored in organic and polymer chemistry.[33, 34] However, care must be taken when choosing those ionic liquids rich in alkyl chains as hindered solvent because the linear alkyl chains of ionic liquids (e.g. [Bmim][NTf_2]) will completely fill the microporous structure of zeolites resulting in loss of the microporous structures (Fig. S1, ESI†).[13] To solve this problem, branched ionic liquids are a potential solution for three key reasons. First, the branched topology and size prevent the ions from entering the zeolite pores completely.[35] Second, one long branched alkyl chain can enter the zeolite channel at the interface and form a mechanical bond. Third, the strength of the hydrogen bonding interaction between the adsorbed alkane chain and the Brønsted sites in the H-form zeolites could be utilized to stabilize this specific organic-inorganic system.[32] Toward this end, a porous liquid zeolite (i.e., H-ZSM-5-liquid/[P66614][Br]) based on H-ZSM-5 nanoparticles (NPs) was designed and fabricated by directly dissolving H-ZSM-5 NPs (Table S1, Fig. S2-S5, ESI†) in branched ionic liquids (i.e., [P66614][Br]) at room temperature (Scheme 1). As shown in Fig. S6, our molecular dynamics (MD) simulations indicate that steric hindrance from the four alkyl chains of $[P66614]^+$ prevents the micropores of H-ZSM-5 NPs from being filled. Hence, the microporous structure in the H-ZSM-5-liquid/[P66614][Br] will remain empty and available for use.

In the beginning, the hydrogen bonding interaction that served to stabilize the H-ZSM-5 NPs in [P66614][Br] the liquid matrix was identified simply by monitoring the solution stability. Fig. 1a presents photographs of H-ZSM-5 NPs, Na-ZSM-5-liquid/[P66614][Br] and H-ZSM-5-liquid/[P66614][Br] in chloroform at a concentration of 5.0 mg mL^{-1}, respectively. It is clear that H-ZSM-5 NPs and Na-ZSM-5-liquid/[P66614][Br] are almost insoluble in chloroform and immediately agglomerate to produce precipitates because neither of them can form hydrogen bonds in chloroform which would stabilize the solution (Fig. S7, ESI†). In contrast, the H-ZSM-5-liquid/[P66614][Br] dissolves well and shows excellent solution stability in chloroform even after 2 h. This expected solution stability corroborates the hydrogen bonding interaction between alkyl chains in the [P66614][Br] and Brønsted sites in the H-ZSM-5 NPs as shown in Fig. 1b and Fig. S4, S5.[32, 36] Because of the presence of hydrogen bonding, [P66614][Br] molecules can strongly attach onto the surface of the H-ZSM-5 NPs, leading to good solubility in chloroform for H-ZSM-5-liquid/[P66614][Br]. Fig. 1c shows a representative model of the interaction between [P66614][Br] and H-ZSM-5 NPs surface based on our MD simulations. One can clearly see the hydrogen bond at the interface: the $H^{\delta+}$ (H-ZSM-5) --- $H^{\delta-}$ (alkyl) distance is approximately 1.9-2.0 Å (Fig. 1d). One can also see from Fig. 1c that some alkyl chains penetrate into the zeolite channels at the interface. This interaction resembles the mechanical bonds (such as in rotaxanes), because the alkyl chains are locked by the narrow windows in the middle but stabilized by their greater entropy at the free ends in the larger cavities. It has been suggested that the alkyl chains could also transfer charge to the H-ZSM-5 NPs,[37] which is beneficial to efficiently balance the van der Waals force and eliminate aggregation of H-ZSM-5-liquid/[P66614][Br] in chloroform. As a result, the H-ZSM-5-liquid/[P66614][Br] can be stably dispersed in chloroform without any evidence of aggregation. Thus, we conclude that H-ZSM-5-liquid/[P66614][Br] is a homogeneous and stable fluid at room temperature (Fig. S8, ESI†).

The viscosity of the H-ZSM-5-liquid/[P66614][Br] was then characterized by a rotation rheometer. As demonstrated in Fig. 2a, the viscosities of this H-ZSM-5-liquid/[P66614][Br] are 9.55 Pa·s at 25 °C and 0.81 Pa·s at 90 °C, respectively, both of which are higher than [P66614][Br] (Fig. S9, ESI†), but still low enough that the H-ZSM-5-liquid/[P66614][Br] behaves like a 'real liquid' and thus exhibits high mobility at room temperature.[38] Fig. S10 displays the thermogravimetric analysis (TGA) of the H-ZSM-5-liquid/[P66614][Br] and [P66614][Br], respectively. It can be easily seen that there is no weight loss below 300 °C, indicating that the H-ZSM-5-liquid/[P66614][Br] does not contain any residual traditional solvent (e.g., water, ethanol, chloroform etc.), thus demonstrating that the H-ZSM-5-

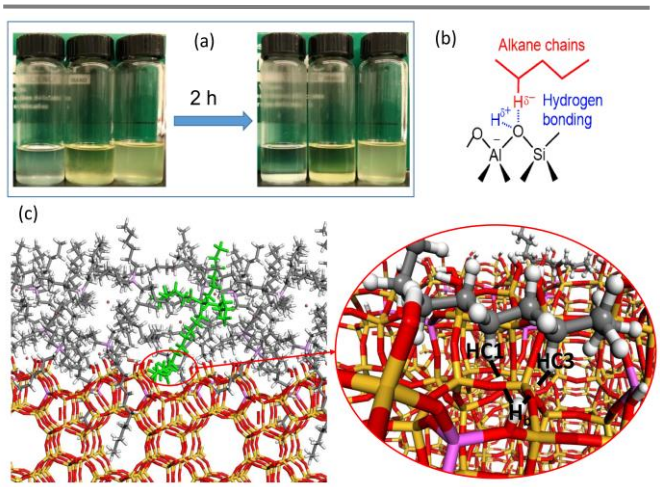

Fig. 1 a) Photographs of H-ZSM-5 NPs (left), Na-ZSM-5-liquid/[P66614][Br] (Middle) and H-ZSM-5-liquid/[P66614][Br] (right) in chloroform, b) The hydrogen bonding interaction between H-ZSM-5 NPs and alkyl chains of [P66614][Br] and c) The snapshot from molecular dynamics simulation showing the hydrogen bonding between [P66614][Br] and the Brønsted site on H-ZSM-5 [100] surface. Color code: Si, yellow; Al, purple; O, red; C, grey; H, white.

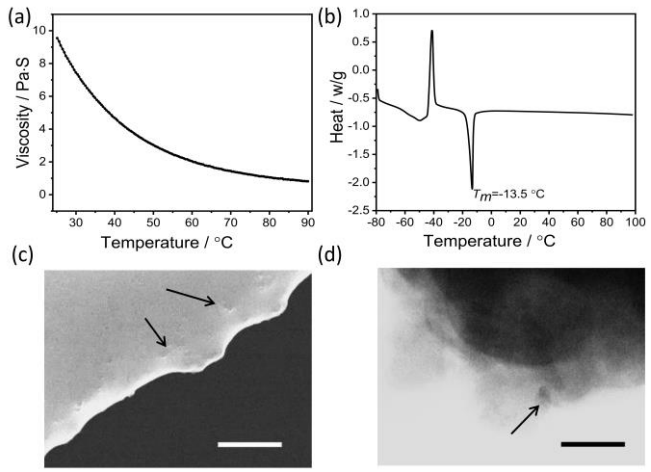

Fig. 2 a) Viscosity versus temperature trace and (b) DSC curve for the H-ZSM-5-liquid/[P66614][Br]; c) SEM (scale bar = 3 μm) and d) TEM images (scale bar = 150 nm) of the H-ZSM-5-liquid/[P66614][Br], respectively. Arrows indicate location of H-ZSM-5 NPs.

liquid/[P66614][Br] is solvent-free. TGA results also show that the organic weight content is approximately 72.7 wt. %, which is high enough to act as the continuous liquid matrix and provide fluidity for the H-ZSM-5 NPs.[38] Differential scanning calorimetry (DSC) results exhibited in Fig. 2b provides information on the physical properties of the H-ZSM-5-liquid/[P66614][Br]. As we can see, the melting temperature (T_m) of the H-ZSM-5-liquid/[P66614][Br] occurs at -13.5 °C, which is well below room temperature, further confirming that the system remains in the melt state and exhibits liquid-like behavior, consistent with its rheological response in Fig. 2a. Scanning electron microscopy (SEM) and transmission electron microscopy (TEM) are also utilized to investigate the microscopic configuration of the H-ZSM-5-liquid/[P66614][Br]. As expected, the SEM image shown in Fig. 2c indicates that the H-ZSM-5-liquid/[P66614][Br] self-assembly becomes a continuous matrix with evidence of the H-ZSM-5 particles dispersed throughout, which is in sharp contrast to that of the H-ZSM-5 NPs (Fig. S11, ESI†). This interesting continuous matrix can be understood by considering the flowability of [P66614][Br]. The attached [P66614][Br] will spontaneously flow and thereby fill out the discontinuous region among H-ZSM-5 NPs.[39, 40] Additionally, the TEM image of H-ZSM-5-liquid/[P66614][Br] (Fig. 2d) suggests that the H-ZSM-5 NPs are dispersed throughout the [P66614][Br] liquid matrix without any significant recombination. The excellent dispersion of the H-ZSM-5 NPs is also derived from the attached [P66614][Br] molecules, which efficiently cover the H-ZSM-5 NPs through the hydrogen bonding interaction and thereby act as physical barriers to lower the contact risk between H-ZSM-5 NPs.[39, 41]

As shown in Fig. 3, the H-ZSM-5-liquid/[P66614][Br] was examined by several characterization techniques. Typical characteristic peaks of both of H-ZSM-5 NPs (e.g., 7.84°, 8.8°, 23.2°, etc, Fig. S2, ESI†) and [P66614][Br] (i.e., 20.8°, Fig. S12, ESI†) were clearly observed in the wide angle x-ray diffraction (XRD) pattern of the H-ZSM-5-liquid/[P66614][Br] as shown in Fig. 3a. This result demonstrates that the crystal structure of H-ZSM-5 NPs has been well preserved in the H-ZSM-5-liquid/[P66614][Br] without collapse.[2] Positron annihilation lifetime spectroscopy (PALS) was used to determine if the pore structure in the H-ZSM-5-liquid remained empty. PALS serves as an accurate probe of the micropore structure by measuring the lifetime of a positron which can be correlated to the average size of micropores in the material. As exhibited in Fig. S13, the o-Ps lifetime measured for H-ZSM-5-liquid was determined to be about 1.012 ns, which corresponds to an average cavity diameter of 3.51 Å based on the well-established Tao-Eldrup model.[42-44] This is slightly less than the pore size of H-ZSM-5 NPs (5.4–5.6 Å) because the attached alkane chains of [P66614][Br] indeed occupy a certain pore space within the H-ZSM-5 NPs, resulting in a slight decrease in the average cavity diameter of the H-ZSM-5-liquid/[P66614][Br], though that empty space remains available for use.[3, 4,45] To further demonstrate the permanent porosity of the H-ZSM-5-liquid/[P66614][Br], its porous structure was characterized by gas adsorption-desorption measurements where the pure [P66614][Br] liquid matrix was employed as the reference sample. As shown in Fig. 3b, the CO_2 sorption capacity of the H-ZSM-5-liquid/[P66614][Br] was larger than the [P66614][Br] over the entire measured pressure range because the permanent porosity present in the H-ZSM-5-liquid/[P66614][Br] could provide additional free volume to accommodate gas molecules (e.g., CO_2), thus leading to a higher gas adsorption capacity.[3, 4, 13] More importantly, in addition to the improvement of gas sorption capacity, the gas adsorption-desorption behavior of H-ZSM-5-liquid/[P66614][Br] with permanent porosity is different from that of [P66614][Br]. For example, the CO_2 adsorption-desorption isotherm of [P66614][Br] is linear while the CO_2 adsorption- desorption isotherm of H-ZSM-5-liquid/[P66614][Br] is nonlinear, similar to the nonlinear adsorption-desorption curve of H-ZSM-5 NPs (Fig. 3b). Finally, H-ZSM-5-

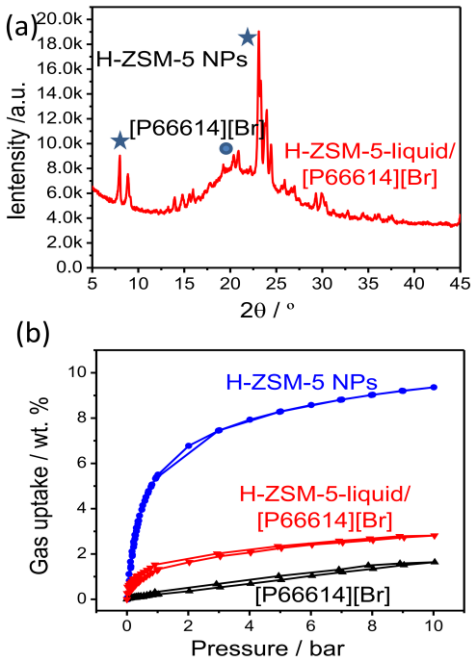

Fig. 3 a) XRD Pattern of H-ZSM-5-liquid/[P66614][Br] (Star: H-ZSM-5 NPs, Circle: [P66614][Br]); b) CO_2 adsorption-desorption isotherms of H-ZSM-5 NPs, [P66614][Br] and H-ZSM-5-liquid/[P66614][Br] collected at 298 K, respectively.

liquid/[P66614][Br] analogues (i.e., H-ZSM-5-liquid/[Aliquant336][Cl] and H-ZSM-5-liquid/[P4442][Suc]) obtained by mixing the same porous host (H-ZSM-5 NPs) with other types of branched ionic liquids (e.g., [Aliquant336][Cl] and [P4442][Suc], Fig. S14, ESI†) using the same methodology were also prepared and measured. As shown in Fig. S15, both of these two H-ZSM-5-liquid/[P66614][Br] analogues exhibited similar non-linear CO_2 adsorption-desorption isotherms, demonstrating the existence of permanent porosity for gas storage. Hence, this strategy based on hydrogen bonding-stabilized H-ZSM-5 NPs in branched ionic liquid is a general and efficient method to fabricate porous liquid zeolites.

Conclusions

In summary, we have developed an efficient and general strategy for the liquefaction of H-form zeolites by the hydrogen bonding interaction between the alkyl chains of branched ionic liquids and Brønsted sites in H-form zeolites enhanced by the interfacial mechanical bonds. The resulting porous liquid zeolites, as expected, are homogeneous and stable fluids at room temperature. XRD pattern, positron annihilation lifetime and gas adsorption-desorption measurements successfully demonstrate the existence of permanent porosity in this hybrid liquid system, which can serve as the free space to host gas molecules, not only significantly improving the gas sorption capacity, but also changing the gas sorption-desorption behaviour. Notably, such a facile synthetic strategy can be further extended to fabricate other types of H-form zeolites-based porous liquids by taking advantage of the tunability of the counter-anion (e.g., NTf_2^-, BF_4^-, $EtSO_4^-$, etc.) in branched ionic liquids and by increasing the mass fraction of the H-form zeolites in the hybrid system, thus paving the way to further optimize their gas sorption performance, as well as opening up new opportunities for porous liquids for utilization in gas capture and other potential applications.

Conflicts of interest

There are no conflicts to declare.

Acknowledgements

This work was supported by the U.S. Department of Energy, Office of Science, Chemical Sciences, Basic Energy Sciences, Geosciences, and Biosciences Division. P. Li also acknowledges the support from the China Scholar Council. Y. Zheng appreciates the financial supports from National Natural Science Foundation of China (No. 51373137), Shaanxi International Science and Technology Cooperation and Exchange Program (No. 2016KW-053), Natural Science Basic Research Plan in Shaanxi Province of China (No. 2017JQ2002).

Notes and references

1. N. O'Reilly, N. Giri and S. L. James, *Chemistry-A European Journal*, 2007, **13**, 3020.
2. J. Zhang, S. H. Chai, Z. A. Qiao, S. M. Mahurin, J. Chen, Y. Fang, S. Wan, K. Nelson, P. Zhang and S. Dai, *Angewandte Chemie International Edition*, 2015, **127**, 946.
3. N. Giri, M. G. Del Pópolo, G. Melaugh, R. L. Greenaway, K. Rätzke, T. Koschine, L. Pison, M. F. C. Gomes, A. I. Cooper and S. L. James, *Nature*, 2015, **527**, 216.
4. P. Li, J. A. Schott, J. Zhang, S. M. Mahurin, Y. Sheng, Z. A. Qiao, X. Hu, G. Cui, D. Yao and S. Brown, *Angewandte Chemie International Edition*, 2017, **129**, 15154.
5. R. L. Greenaway, D. Holden, E. G. Eden, A. Stephenson, C. W. Yong, M. J. Bennison, T. Hasell, M. E. Briggs, S. L. James and A. I. Cooper, *Chemical Science*, 2017, **8**, 2640.
6. F. Zhang, F. Yang, J. Huang, B. G. Sumpter and R. Qiao, *The Journal of Physical Chemistry B*, 2016, **120**, 7195.
7. M. Mastalerz, *Nature*, 2015, **527**, 174.
8. S. L. James, *Advanced Materials*, 2016, **28**, 5712.
9. S. Dai, S. M. Mahurin and J. Zhang, Oak Ridge National Lab.(ORNL), Oak Ridge, TN (United States), 2017.
10. T. M. Swager and V. Schröder, *Synfacts*, 2016, **12**, 0147-0147.
11. A. I. Cooper, *ACS Central Science*, 2017, **3**, 544.
12. T. Shi, Y. Zheng, T. Wang, P. Li, Y. Wang and D. Yao, *ChemPhysChem*, 2018, **19**, 130.
13. W. Shan, P. F. Fulvio, L. Kong, J. Schott, C.-L. Do-Thanh, T. Tian, X. Hu, S. M. Mahurin, H. Xing and S. Dai, *ACS applied materials & interfaces*, 2018, **10**, 32.
14. N. Giri, C. E. Davidson, G. Melaugh, M. G. Del Pópolo, J. T. Jones, T. Hasell, A. I. Cooper, P. N. Horton, M. B. Hursthouse and S. L. James, *Chemical Science*, 2012, **3**, 2153.
15. M. Costa Gomes, L. Pison, C. Červinka and A. Padua, *Angewandte Chemie International Edition, 10.1002/anie.201805495.*
16. R. Gaillac, P. Pullumbi, K. A. Beyer, K. W. Chapman, D. A. Keen, T. D. Bennett and F.-X. Coudert, *Nature materials*, 2017, **16**, 1149.
17. S. Horike and S. Kitagawa, *Nature materials*, 2017, **16**, 1054.
18. J. Liu, N. Wang, Y. Yu, Y. Yan, H. Zhang, J. Li and J. Yu, *Science Advances*, 2017, **3**, 1603171.
19. N. Wang, Q. Sun, R. Bai, X. Li, G. Guo and J. Yu, *Journal of the American Chemical Society*, 2016, **138**, 7484.
20. G. Feng, P. Cheng, W. Yan, M. Boronat, X. Li, J.-H. Su, J. Wang, Y. Li, A. Corma and R. Xu, *Science*, 2016, **351**, 1188.
21. L. Liu, U. Díaz, R. Arenal, G. Agostini, P. Concepción and A. Corma, *Nature materials*, 2017, **16**, 132.
22. P. J. Bereciartua, Á. Cantín, A. Corma, J. L. Jordá, M. Palomino, F. Rey, S. Valencia, E. W. Corcoran, P. Kortunov and P. I. Ravikovitch, *Science*, 2017, **358**, 1068.
23. M. Moliner, C. Martínez and A. Corma, *Angewandte Chemie International Edition*, 2015, **54**, 3560.
24. R. Bai, Q. Sun, N. Wang, Y. Zou, G. Guo, S. Iborra, A. Corma and J. Yu, *Chemistry of Materials*, 2016, **28**, 6455.
25. Q. Lin, X. Bu, C. Mao, X. Zhao, K. Sasan and P. Feng, *Journal of the American Chemical Society*, 2015, **137**, 6184.
26. H. Awala, J.-P. Gilson, R. Retoux, P. Boullay, J.-M. Goupil, V. Valtchev and S. Mintova, *Nature materials*, 2015, **14**, 447.
27. M. P. Singh, R. K. Singh and S. Chandra, *Progress in Materials Science*, 2014, **64**, 73.
28. Y. Yu, J. Mai, L. Wang, X. Li, Z. Jiang and F. Wang, *Scientific reports*, 2014, **4**, 5997.
29. P. A. Jacobs and R. Von Ballmoos, *The Journal of Physical Chemistry*, 1982, **86**, 3050.
30. H. Zhang, K. Dasbiswas, N. B. Ludwig, G. Han, B. Lee, S. Vaikuntanathan and D. V. Talapin, *Nature*, 2017, **542**, 328.
31. M. Yang, S. Li, Y. Wang, J. A. Herron, Y. Xu, L. F. Allard, S. Lee, J. Huang, M. Mavrikakis and M. Flytzani-Stephanopoulos, *Science*, 2014, **346**, 1498.
32. Y.-H. Yeh, R. J. Gorte, S. Rangarajan and M. Mavrikakis, *The Journal of Physical Chemistry C*, 2016, **120**, 12132.
33. Z. Niu and H. W. Gibson, *Chemical Reviews*, 2009, **109**, 6024.
34. J. F. Stoddart, *Chemical Society Reviews*, 2009, **38**, 1802.

35. H. A. Kalviri and F. M. Kerton, *Advanced Synthesis & Catalysis*, 2011, **353**, 3178.
36. D. Parmar, E. Sugiono, S. Raja and M. Rueping, *Chemical reviews*, 2014, **114**, 9047.
37. Y. Yang, F. Lin, H. Tran and Y. H. C. Chin, *ChemCatChem*, 2017, **9**, 287.
38. Q. Li, L. Dong, W. Deng, Q. Zhu, Y. Liu and C. Xiong, *Journal of the American Chemical Society*, 2009, **131**, 9148.
39. P. Li, Y. Zheng, T. Shi, Y. Wang, M. Li, C. Chen and J. Zhang, *Carbon*, 2016, **96**, 40.
40. Q. Li, L. Dong, F. Sun, J. Huang, H. Xie and C. Xiong, *Chemistry-A European Journal*, 2012, **18**, 7055.
41. N. J. Fernandes, T. J. Wallin, R. A. Vaia, H. Koerner and E. P. Giannelis, *Chemistry of Materials*, 2013, **26**, 84.
42. L. Starannikova, N. Belov, V. Shantarovich, J. Zhang, J. Jin and Y. Yampolskii, *Journal of Membrane Science*, 2018, **548**, 593.
43. C. Li, B. Zhao, B. Zhou, N. Qi, Z. Chen and W. Zhou, *Physical Chemistry Chemical Physics*, 2017, **19**, 7659.
44. A. Zubiaga, R. Warringham, S. Mitchell, L. Gerchow, D. Cooke, P. Crivelli and J. Pérez-Ramírez, *ChemPhysChem*, 2017, **18**, 470.
45. C. R. A. Catlow, R. G. Bell, J. D. Gale and D. W. Lewis, *Studies in Surface Science & Catalysis*, 1995, **97**, 87.

Nanoscale

COMMUNICATION

TOC Graphic:

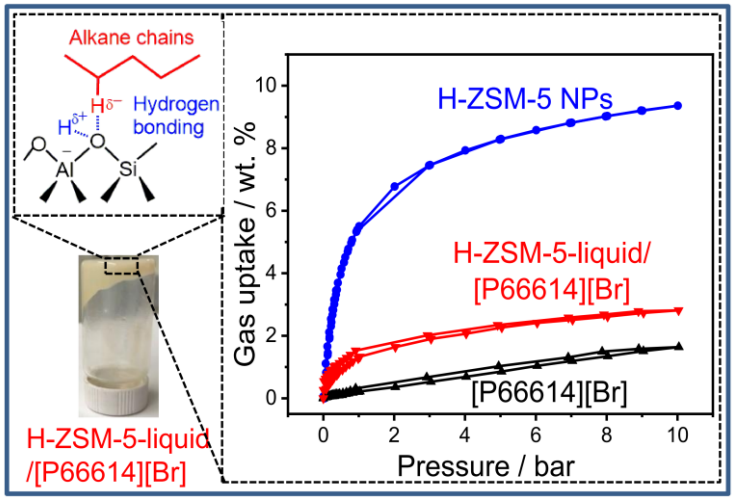

By exploiting the hydrogen bonding interaction between the alkane chains of branched ionic liquids and the Brønsted sites in H-form zeolites, we demonstrate that H-form zeolites-based porous nanoarchitectures can be well stabilized in branched ionic liquids to afford permanent porosity, and thus opens up a novel approach to prepare porous liquid zeolites.